

High-Pressure Vapor–Liquid Equilibria of Some Carbon Dioxide + Organic Binary Systems

Michael J. Lazzaroni, David Bush, James S. Brown, and Charles A. Eckert*

School of Chemical & Biomolecular Engineering and Specialty Separations Center,
Georgia Institute of Technology, Atlanta, Georgia 30332-0100

Vapor–liquid equilibria, molar volumes, and volume expansion for several binary mixtures of organic solvents with carbon dioxide have been determined using a visual synthetic technique at temperatures from (298 to 333) K. The binary vapor–liquid equilibrium and saturated liquid molar volume of CO₂ + acetone, + acetonitrile, + dichloromethane, + nitromethane, + *N*-methyl-2-pyrrolidone, + perfluorohexane, + 2-propanol, + tetrahydrofuran, + toluene, and + 2,2,2-trifluoroethanol were measured at temperatures from (298.2 to 333.2) K. The VLE correlated well using the Patel–Teja equation of state with Mathias–Klotz–Prausnitz mixing rules. The solubility of CO₂ in the various solvents is explained by considering the intermolecular interactions of CO₂ in solution.

Introduction

Carbon dioxide is an interesting process solvent because it is nonflammable, inexpensive, nontoxic, and miscible with many organic solvents. There has been recent interest in the use of carbon dioxide as an antisolvent for the crystallization of dissolved solutes. The choice of solvent in an antisolvent process is a key factor in controlling the solubility of the solute and particle morphology and size.¹ Furthermore, CO₂-expanded solvents as a medium for homogeneously² and heterogeneously³ catalyzed reactions have the potential advantage of increasing solubility and enhancing the mass transfer of gaseous reactants. Carbon dioxide can also aid in the recycling of homogeneous catalysts by effecting a phase split in miscible water + organic + catalyst systems.⁴ All of these applications require knowledge of the vapor–liquid phase behavior and density of the carbon dioxide and organic solvent system to select both the best applicable solvent system and optimum operating conditions. To this end, we have measured the vapor–liquid equilibria of CO₂ + several organic solvents of industrial interest and of varying structure and polarity to develop an understanding of the behavior of CO₂ in solution. The method presented here allows quick and facile measurement of the VLE and PVT properties of dense gases + organic solvents. The binary vapor–liquid equilibrium and liquid density of CO₂ + acetone, + acetonitrile, + dichloromethane, + nitromethane, + *N*-methyl-2-pyrrolidone, + perfluorohexane, + 2-propanol, + tetrahydrofuran, + toluene, and + 2,2,2-trifluoroethanol were measured at temperatures from (298.2 to 333.2) K. The data were correlated with the Patel–Teja cubic equation of state (PT-EoS)⁵ with the Mathias–Klotz–Prausnitz (MKP) mixing rules.⁶

Experimental Methods

Materials. HPLC-grade 2-propanol (99%), acetone (99%), acetonitrile (99%), dichloromethane (99%), nitromethane (99%), *N*-methylpyrrolidone (99%), tetrahydrofuran (99%), toluene (99%), 2,2,2-trifluoroethanol (98%), and perfluoro-

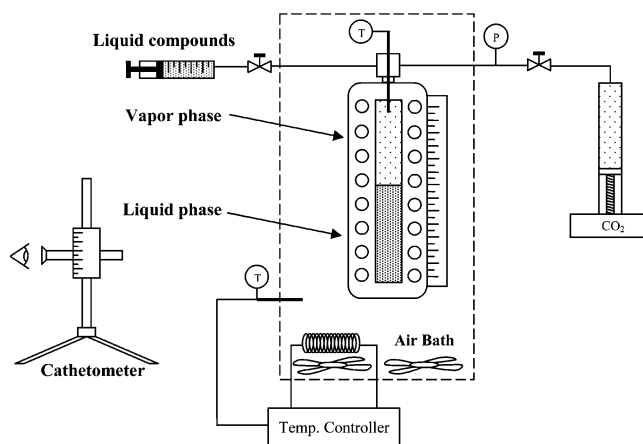


Figure 1. Schematic of equilibrium cell apparatus.

hexane (99%) were obtained from Aldrich Chemical Co. and were used as received. SFC-grade carbon dioxide (99.99%) was obtained from Matheson Gas Products. The CO₂ was further purified to remove trace water using a Matheson (model 450B) gas purifier and filter cartridge (type 451).

Apparatus. Figure 1 shows a schematic of the equilibrium cell apparatus. The equilibrium cell is a transmission-type sight gauge (Jerguson model 18T-32). The working volume of the cell is 150 cm³, which was measured by adding a known amount of gas to the cell at constant temperature and measuring the resulting pressure. The volume scale on the sight gauge was calibrated by adding known volumes of water and measuring the resulting height to increments of 1.6 mm using the fixed scale and measuring any additional height less than the 1.6-mm mark using a cathetometer readable to 0.005 mm. The equilibrium cell was placed in a temperature-controlled air bath. The temperature of the air bath and vapor phase inside the cell was monitored with a thermocouple (Omega Type K) and digital readout (HH-22 Omega). The air bath temperature was maintained by a digital temperature controller (Omega CN76000) with an over-temperature controller (Omega CN375) for safe operation. The temper-

* Corresponding author. E-mail: cac@che.gatech.edu.

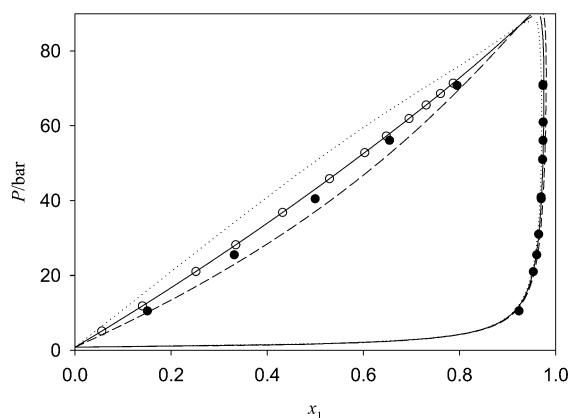


Figure 2. Vapor–liquid equilibria of CO₂ (1) + acetone (2) at 323 K, experimental data, and Patel–Teja EoS prediction: O, this work; ●, Bamberger and Maurer;¹⁴ ···, $k_{ij} = 0.045$; –, $k_{ij} = 0.005$, - · - ·, $k_{ij} = -0.05$.

ature uncertainty was ± 0.2 K and was calibrated against a platinum RTD (Omega PRP-4) with a DP251 Precision RTD Benchtop Thermometer (DP251 Omega) accurate to ± 0.025 K and traceable to NIST. The pressures were measured with a pressure transducer and digital readout (Druck, DPI 260, PDCR 910). The transducer was calibrated against a hydraulic piston pressure gauge (Ruska) to an uncertainty of ± 0.1 bar. The cell is mounted on a rotating shaft, and mixing is achieved by rotating the entire cell.

Experimental Procedure. After the cell was evacuated, the liquid compounds were added to the cell using a gastight syringe. The syringe was weighed before and after liquid addition to find the mass added, which had an estimated uncertainty of less than ± 0.05 g or less than $\pm 0.1\%$ of the mass loaded. CO₂ was added to the cell from a syringe pump (Isco model 260D) operated at a constant pressure using the internal controller and at constant temperature by circulating ethylene glycol from a chiller bath (VWR model 1140) through the external pump jacket. Using the volume displacement of the syringe pump and the density calculated from the Span–Wagner EoS,⁷ the moles of CO₂ added to the cell is calculated with an uncertainty of ± 0.001 mole or, for the smallest loading, an error of $\pm 1.5\%$ in moles added. The cell was rocked vigorously for 5 min and allowed to equilibrate (i.e., no change in temperature, pressure, or volume of the phases). The liquid volume was calculated by measuring the height of the meniscus with a fixed rule, and the differences, with a micrometer cathetometer. For displacements of less than 50 mm, the accuracy is 0.01 mm; for larger displacements, the accuracy is 0.1 mm. The uncertainty in the volume measurement is estimated to be ± 0.2 mL.

Data Reduction. Equilibrium compositions were calculated from the measurements of charge composition and total vapor volume at constant temperature and pressure with the Patel–Teja EoS representing both phases. This approach is commonly referred as the *PTx* method,⁸ and we have chosen the PT-EoS because it gives better predictions of molar volume than the Peng–Robinson or Soave–Redlich–Kwong equations.⁵ With binary interaction parameters set to 0, we perform a flash calculation at fixed temperature and pressure to get estimates of the liquid- and vapor-phase concentrations and density. As shown in Figure 2, the liquid-phase concentration is sensitive to large changes in the interaction parameter, whereas the vapor-phase concentration is insensitive. The vapor concentration

Table 1. Pure-Component Parameters Used in the Patel–Teja EoS^a

compound	T_c /K	P_c /MPa	Z	F
acetone	508.2	4.70	0.2819	0.7085
acetonitrile	545.5	4.83	0.2240	0.4780
carbon dioxide	304.2	7.36	0.3106	0.7115
dichloromethane	510	6.08	0.2950	0.6320
nitromethane	588.2	6.31	0.2633	0.6593
<i>N</i> -methyl-2-pyrrolidone	721.6	4.52	0.2768	0.7536
perfluorohexane	451	1.86	0.3160	1.1185
2-propanol	508.3	4.76	0.3001	1.2814
tetrahydrofuran	540.2	5.19	0.3112	0.7266
toluene	591.8	4.11	0.3080	0.7708
2,2,2-trifluoroethanol	499	4.87	0.2952	1.2229

^a Critical temperature and pressure are from the DIPPR database.¹³ Z and F were calculated to match density and vapor pressure data taken from the DIPPR database.

Table 2. Binary Interaction Parameters for CO₂ + Organic Compounds for MKP with the Patel–Teja EoS

compound	$k_{ij}^{(0)}$	$k_{ij}^{(1)}/K$	$l_{ij}^{(0)}$	$l_{ij}^{(1)}/K$
acetone	-0.005		0	
acetonitrile	-0.043		-0.074	
dichloromethane	0.046		0	
nitromethane	0.098	-33	0.318	-102
<i>N</i> -methyl-2-pyrrolidone	-0.012		0.005	
perfluorohexane	0.057		-0.069	
2-propanol	0.119		0.030	
tetrahydrofuran	0.137	-40	0.560	-173
toluene	0.099		0.056	
2,2,2-trifluoroethanol	0.156	-28	0.373	-122

Table 3. Composition, Pressure, Molar Volume, and Volume Expansion of Carbon Dioxide (1) + 2-Propanol (2) at 313 K

T/K	P/bar	x_1	$y_{1,\text{calcd}}$	$v_m^L/\text{cm}^3\cdot\text{mol}^{-1}$	$\Delta V/\%$
313	7.2	0.018	0.954	79.7	3
313	16.5	0.065	0.984	78.8	7
313	26.6	0.133	0.990	76.2	12
313	36.9	0.210	0.992	74.5	20
313	47.2	0.300	0.992	71.7	30
313	56.7	0.401	0.992	68.5	45
313	62.6	0.510	0.991	64.0	65
313	69.4	0.639	0.989	60.6	111
313	73.0	0.725	0.989	59.9	174
313	75.8	0.788	0.988	60.1	258

Table 4. Composition, Pressure, Molar Volume, and Volume Expansion of Carbon Dioxide (1) + Acetonitrile (2) at 313 K

T/K	P/bar	x_1	$y_{1,\text{calcd}}$	$v_m^L/\text{cm}^3\cdot\text{mol}^{-1}$	$\Delta V/\%$
313	2.1	0.044	0.926	51.9	1
313	4.6	0.073	0.954	52.5	5
313	6.2	0.093	0.964	53.3	9
313	13.1	0.168	0.979	52.4	16
313	20.1	0.241	0.985	51.1	24
313	27.0	0.312	0.988	51.0	37
313	33.8	0.381	0.989	51.8	54
313	40.8	0.449	0.990	50.7	69
313	47.7	0.523	0.990	49.8	91
313	54.3	0.598	0.990	49.6	126
313	61.5	0.688	0.989	49.0	186
313	67.6	0.770	0.989	48.7	285
313	72.5	0.834	0.988	50.8	454

and density are used to obtain a corrected liquid-phase concentration using eq 1.

$$x_i = \frac{n_i^{\text{tot}} - y_{i,\text{EoS}} V_{\text{exptl}}^V \rho_{\text{EoS}}^V}{n^{\text{tot}} - V_{\text{exptl}}^V \rho_{\text{EoS}}^V} \quad (1)$$

where n is the number of moles, y is the vapor mole

Table 5. Composition, Pressure, Molar Volume, and Volume Expansion of Carbon Dioxide (1) + Dichloromethane (2) at 313 K

<i>T/K</i>	<i>P/bar</i>	x_1	$y_{1,calcd}$	$v_m^L/cm^3 \cdot mol^{-1}$	$\Delta V/\%$
313	5.5	0.044	0.799	65.1	2
313	12.4	0.114	0.906	63.2	7
313	19.2	0.188	0.937	62.4	15
313	26.3	0.269	0.952	61.3	26
313	40.1	0.444	0.965	58.7	58
313	46.6	0.533	0.968	57.4	83
313	53.4	0.644	0.971	56.4	135
313	60.2	0.738	0.973	53.2	202
313	66.8	0.830	0.974	54.2	380
313	69.5	0.859	0.975	58.2	526

Table 6. Composition, Pressure, Molar Volume, and Volume Expansion of Carbon Dioxide (1) + Nitromethane (2) at 298 K

<i>T/K</i>	<i>P/bar</i>	x_1	$y_{1,calcd}$	$v_m^L/cm^3 \cdot mol^{-1}$	$\Delta V/\%$
298	8.9	0.120	0.994	49.3	9
298	18.5	0.238	0.997	48.3	24
298	26.9	0.346	0.997	47.6	42
298	35.2	0.457	0.998	47.4	71
298	41.4	0.552	0.998	47.4	107
298	48.3	0.678	0.998	47.1	185
298	51.4	0.747	0.998	47.7	267
298	54.3	0.810	0.998	47.8	391
298	55.7	0.855	0.998	48.7	558
298	56.6	0.876	0.998	49.1	671

Table 7. Composition, Pressure, Molar Volume, and Volume Expansion of the Carbon Dioxide + Nitromethane System at 313 K

<i>T/K</i>	<i>P/bar</i>	x_1	$y_{1,calcd}$	$v_m^L/cm^3 \cdot mol^{-1}$	$\Delta V/\%$
313	5.0	0.048	0.979	58.8	6
313	12.4	0.119	0.990	57.1	12
313	19.2	0.183	0.993	55.6	17
313	26.8	0.254	0.994	55.1	27
313	33.2	0.320	0.995	54.5	38
313	39.9	0.385	0.995	53.7	50
313	49.0	0.479	0.995	53.2	76
313	55.2	0.546	0.995	52.3	98
313	61.6	0.627	0.995	50.9	134
313	67.9	0.727	0.994	49.9	214
313	71.7	0.791	0.994	50.8	318

Table 8. Composition, Pressure, Molar Volume, and Volume Expansion of Carbon Dioxide (1) + N-Methyl-2-pyrrolidone (2) at 313 K

<i>T/K</i>	<i>P/bar</i>	x_1	$y_{1,calcd}$	$v_m^L/cm^3 \cdot mol^{-1}$	$\Delta V/\%$
313	7.2	0.104	0.9997	89.1	2
313	15.4	0.190	0.9998	84.8	7
313	20.6	0.242	0.9998	82.6	12
313	28.1	0.311	0.9998	79.0	18
313	35.2	0.374	0.9998	75.7	24
313	41.9	0.437	0.9998	73.2	33
313	48.9	0.499	0.9998	69.8	43
313	56.0	0.565	0.9998	66.6	57
313	62.5	0.629	0.9997	62.3	73
313	69.4	0.725	0.9995	56.7	111
313	77.8	0.816	0.9991	53.4	197

fraction, V is the total volume, and ρ is the molar density. The interaction parameters for the MKP mixing rules, as shown in eqs 2 and 3, are then regressed to minimize $\sum_i(x_i - x_{i,EoS})^2$ for each isotherm.

$$a = \sum_i x_i \sum_j x_j a_{ji}^{(0)} (1 - k_{ij}) + \sum_i x_i \left(\sum_j x_j (a_{ji}^{(0)} l_{ij}^{(1)})^{1/3} \right)^3 \quad (2)$$

$$a_{ji}^{(0)} = \sqrt{a_i a_j} \quad (3)$$

Where data are measured over a temperature range, the

Table 9. Composition, Pressure, Molar Volume, and Volume Expansion of Carbon Dioxide (1) + Tetrahydrofuran (2) at 298 K

<i>T/K</i>	<i>P/bar</i>	x_1	$y_{1,calcd}$	$v_m^L/cm^3 \cdot mol^{-1}$	$\Delta V/\%$
298	6.6	0.132	0.967	70.8	4
298	11.7	0.228	0.981	65.5	8
298	17.6	0.333	0.987	64.6	24
298	25.0	0.451	0.990	62.0	44
298	29.4	0.518	0.991	60.8	61
298	36.1	0.624	0.993	58.6	98
298	42.8	0.736	0.994	56.4	173
298	49.2	0.830	0.995	54.9	312
298	53.8	0.899	0.996	54.3	590

Table 10. Composition, Pressure, Molar Volume, and Volume Expansion of Carbon Dioxide (1) + Tetrahydrofuran (2) at 313 K

<i>T/K</i>	<i>P/bar</i>	x_1	$y_{1,calcd}$	$v_m^L/cm^3 \cdot mol^{-1}$	$\Delta V/\%$
313	7.1	0.098	0.940	77.5	5
313	23.2	0.313	0.978	70.9	26
313	29.7	0.398	0.982	68.2	38
313	36.8	0.489	0.985	65.3	55
313	44.2	0.576	0.986	62.9	80
313	50.7	0.655	0.987	62.3	119
313	57.5	0.733	0.988	60.2	174
313	65.2	0.832	0.989	57.2	312
313	71.4	0.890	0.989	60.2	574

Table 11. Composition, Pressure, Molar Volume, and Volume Expansion of Carbon Dioxide (1) + Tetrahydrofuran (2) at 333 K

<i>T/K</i>	<i>P/bar</i>	x_1	$y_{1,calcd}$	$v_m^L/cm^3 \cdot mol^{-1}$	$\Delta V/\%$
333	16.0	0.165	0.942	74.5	12
333	25.0	0.260	0.958	73.4	24
333	40.1	0.404	0.968	68.7	43
333	55.0	0.539	0.972	66.0	76
333	69.9	0.696	0.973	58.4	133
333	84.7	0.808	0.971	60.4	272
333	90.1	0.850	0.969	62.9	390
333	95.4	0.893	0.964	70.5	690

Table 12. Composition, Pressure, Molar Volume, and Volume Expansion of Carbon Dioxide (1) + 2,2,2-Trifluoroethanol (2) at 298 K

<i>T/K</i>	<i>P/bar</i>	x_1	$y_{1,calcd}$	$v_m^L/cm^3 \cdot mol^{-1}$	$\Delta V/\%$
298	11.3	0.132	0.990	63.9	9
298	20.5	0.225	0.994	63.0	20
298	31.2	0.358	0.995	59.5	37
298	40.6	0.480	0.995	58.1	65
298	47.4	0.599	0.995	57.1	110
298	51.8	0.704	0.995	55.1	174
298	53.4	0.749	0.995	55.1	223
298	55.1	0.795	0.995	54.3	290
298	56.6	0.842	0.995	54.9	410
298	57.9	0.888	0.996	54.8	624
298	59.5	0.927	0.996	55.0	1014

following temperature dependency of the interaction parameters is used:

$$k_{ij} = k_{ij}^{(0)} + \frac{k_{ij}^{(1)}}{T} \quad (4)$$

$$l_{ij} = l_{ij}^{(0)} + \frac{l_{ij}^{(1)}}{T} \quad (5)$$

The PT-EoS pure-component parameters are shown in Table 1, and the binary interaction parameters for the MKP mixing rules are shown in Table 2.

The method presented here is similar to previously published visual synthetic techniques, where typically the vapor phase is assumed to contain none of the organic

Table 13. Composition, Pressure, Molar Volume, and Volume Expansion of Carbon Dioxide (1) + 2,2,2-Trifluoroethanol (2) at 313 K

<i>T</i> /K	<i>P</i> /bar	<i>x</i> ₁	<i>y</i> _{1,calcd}	<i>v</i> _m ^L /cm ³ ·mol ⁻¹	Δ <i>V</i> /%
313	18.2	0.160	0.985	61.0	14
313	25.9	0.230	0.988	61.3	25
313	37.7	0.337	0.990	60.6	43
313	46.6	0.424	0.990	59.4	60
313	55.0	0.517	0.990	58.4	87
313	62.8	0.628	0.990	55.1	127
313	67.3	0.715	0.989	53.0	183
313	70.9	0.773	0.988	53.4	256
313	75.0	0.849	0.988	56.5	468
313	77.5	0.901	0.987	59.8	828

Table 14. Composition, Pressure, Molar Volume, and Volume Expansion of Carbon Dioxide (1) + Perfluorohexane (2) at 313 K

<i>T</i> /K	<i>P</i> /bar	<i>x</i> ₁	<i>y</i> _{1,calcd}	<i>v</i> _m ^L /cm ³ ·mol ⁻¹	Δ <i>V</i> /%
313	6.9	0.146	0.928	186.7	1
313	12.1	0.163	0.935	187.0	2
313	14.5	0.270	0.958	173.2	5
313	17.2	0.262	0.957	174.2	11
313	22.5	0.339	0.965	165.5	13
313	27.7	0.424	0.970	151.1	20
313	32.8	0.474	0.972	144.8	27
313	37.9	0.547	0.974	132.4	37
313	43.2	0.615	0.975	123.5	38
313	48.6	0.665	0.975	116.5	51
313	53.3	0.721	0.975	106.2	68
313	55.9	0.765	0.974	97.0	86
313	58.6	0.776	0.974	94.9	93
313	62.0	0.811	0.973	90.3	123
313	64.2	0.836	0.973	91.7	168

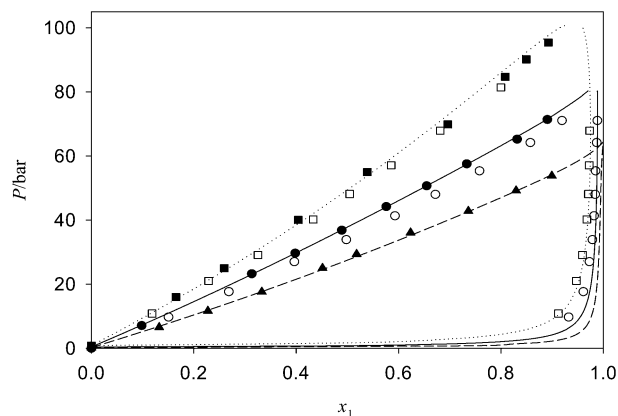
Table 15. Composition, Pressure, Molar Volume, and Volume Expansion of Carbon Dioxide (1) + Acetone (2) at 323 K

<i>T</i> /K	<i>P</i> /bar	<i>x</i> ₁	<i>y</i> _{1,calcd}	<i>v</i> _m ^L /cm ³ ·mol ⁻¹	Δ <i>V</i> /%
323	4.9	0.056	0.835	73.7	4
323	11.1	0.140	0.924	71.8	11
323	20.0	0.251	0.953	67.5	19
323	27.4	0.335	0.962	66.7	33
323	36.3	0.432	0.969	64.2	49
323	45.9	0.530	0.972	62.3	74
323	53.6	0.603	0.974	61.0	102
323	58.1	0.648	0.975	60.1	124
323	63.0	0.695	0.975	57.1	146
323	65.2	0.730	0.975	56.6	177
323	67.8	0.760	0.975	57.4	216
323	71.1	0.787	0.975	58.1	260

Table 16. Composition, Pressure, Molar Volume, and Volume Expansion of Carbon Dioxide (1) + Toluene (2) at 323 K

<i>T</i> /K	<i>P</i> /bar	<i>x</i> ₁	<i>y</i> _{1,calcd}	<i>v</i> _m ^L /cm ³ ·mol ⁻¹	Δ <i>V</i> /%
323	12.0	0.091	0.987	101.4	2
323	21.2	0.175	0.991	97.2	7
323	31.5	0.260	0.993	92.1	13
323	40.1	0.335	0.993	87.6	19
323	48.1	0.408	0.993	83.7	28
323	55.4	0.480	0.993	80.2	39
323	59.6	0.524	0.992	78.2	48
323	63.1	0.583	0.992	72.2	55
323	67.2	0.644	0.991	67.2	69
323	73.8	0.715	0.990	64.6	101
323	78.0	0.764	0.989	63.2	137
323	82.1	0.821	0.988	62.3	206
323	85.0	0.865	0.986	62.6	309
323	86.6	0.883	0.986	63.5	383

component and the density or volume of the liquid phase is measured.^{9,10} For the solvents in this study, the predicted mole fraction in the vapor phase ranged from 0.01 to 0.05, which improves the accuracy of eq 1. From the propagation

**Figure 3.** Comparison of *Pxy* diagram of CO₂ (1) + tetrahydrofuran (2): ▲, 298 K; ●, 313 K; ■, 333 K; this work; ○, 311.01 K, this work; □, 331.33 K, Im et al.;¹⁵ lines are the Patel–Teja EoS.

of uncertainties in eq 1, we estimate the uncertainty in liquid composition to be ±2.8%.

The molar volume of the liquid phase (*v*_m^L) is calculated from eq 6

$$v_m^L = \frac{V_{\text{exptl}}^L}{n^{\text{tot}} - V_{\text{exptl}}^V \rho_{\text{EoS}}^V} \quad (6)$$

where *V*_{exptl}^L is the experimentally measured volume of the liquid phase and the denominator is the calculated number of moles in the liquid phase. The estimated uncertainty is 2.6%. The volume expansion of the liquid phase is defined as the change in total volume divided by the volume of the pure organic solvent liquid, as shown in eq 7.

$$\frac{V_{\text{exptl}}^L(T, P, x_1) - V_2^L(T, P^0)}{V_2^L(T, P^0)} = \Delta V \quad (7)$$

where *V*_{exptl}^L is the total volume of the liquid phase and *V*₂^L is the total volume of the pure solvent at the same temperature and atmospheric pressure.¹¹

Results and Discussion

The binary vapor–liquid equilibrium and liquid density of CO₂ + acetonitrile, + dichloromethane, + *N*-methyl-2-pyrrolidone, + perfluorohexane, and + 2-propanol were measured at 313.2 K, CO₂ + nitromethane and CO₂ + 2,2,2-trifluoroethanol at 298.2 K and 313.2 K, CO₂ + tetrahydrofuran at 298.2 K, 313.2 K, and 333.2 K, and CO₂ + acetone and CO₂ + toluene at 323.2 K. The data are shown in Tables 3 to 16. Isothermal *Pxy* data for CO₂ + THF using this technique, shown in Figure 3, are in good agreement with literature data, with deviations of less than 5% in mole fraction. A comparison of molar volumes for CO₂ + acetonitrile and CO₂ + 2-propanol, as shown in Figure 4, are in good agreement with densitometer measurements, with differences of less than 2%.

Considering the solubility of CO₂ in a series of polar organic solvents as shown in Figure 5, some interesting behavior can be seen. The solubility of CO₂ at an arbitrary pressure of 50 bar is from most soluble to least soluble perfluorohexane, tetrahydrofuran, dichloromethane, acetonitrile, *N*-methyl-2-pyrrolidone, nitromethane, 2,2,2-trifluoroethanol, and 2-propanol. The high solubility of carbon dioxide in perfluorohexane is expected because it is known to be very soluble in fluorinated compounds because they have similar low cohesive energy densities. THF has a

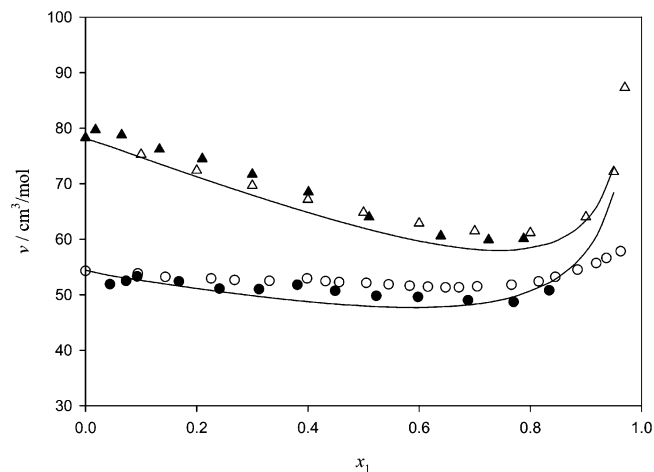


Figure 4. Molar volume of CO₂ (1) + acetonitrile (2) (●, this work; ○, Kordikowski et al.¹⁶) and CO₂ (1) + 2-propanol (2) at 313 K (▲, this work; △, Yaginuma et al.¹⁷); lines are the Patel–Teja EoS.

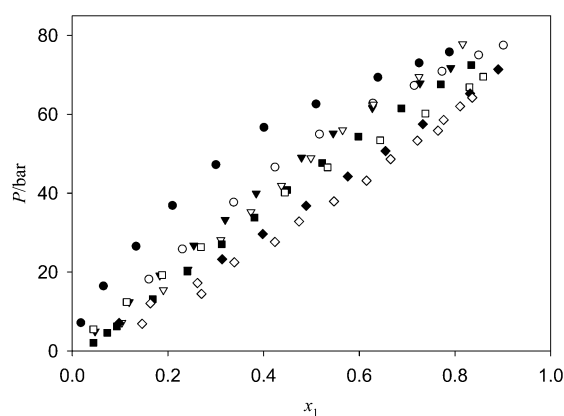


Figure 5. P - x diagram of carbon dioxide (1) + organic solvent (2) at 313 K: ●, 2-propanol; ○, TFE; ▼, nitromethane; ▽, NMP; ■, acetonitrile; □, dichloromethane; ◆, THF; ◇, perfluorohexane.

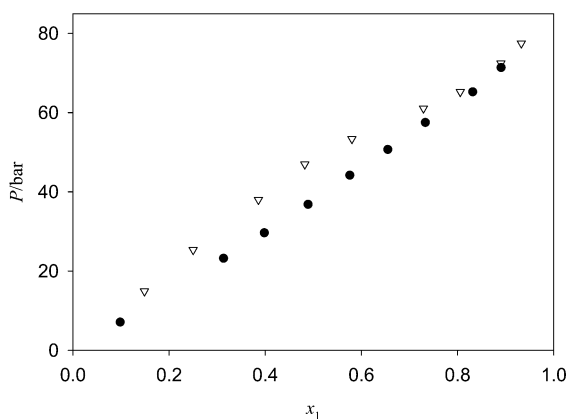


Figure 6. Comparison of P - x diagram at 313 K for CO₂ (1) + tetrahydrofuran (2), ●, this work and CO₂ (1) + benzene (2), ▽, Ohgaki and Katayama.¹⁸

similar Kamlet–Taft solvatochromic polarizability/dipolarity parameter to that of benzene ($\pi^* = 0.58$ to $\pi^* = 0.59$), and comparing the solubility of CO₂ in THF to its solubility in benzene, as can be seen in Figure 6, we see a higher solubility in THF. We assume the CO₂ acts as a Lewis acid and can interact with the basic ether functionality of THF but less so with the similarly structured and much less basic aromatic ring of benzene. Although CO₂ has a zero net dipole moment, the high solubility of carbon dioxide in polar solvents such as acetonitrile and nitromethane at-

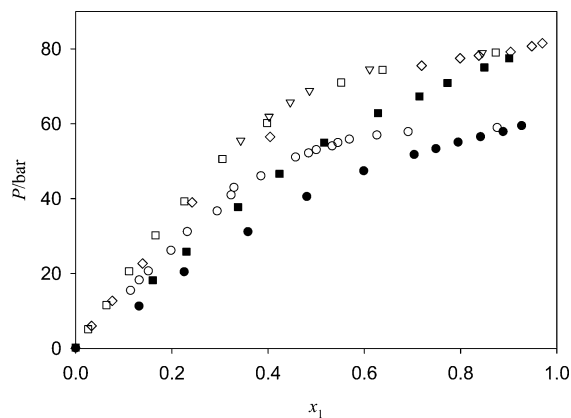


Figure 7. Comparison of the P - x diagrams of CO₂ (1) + 2,2,2-trifluoroethanol (2) (●, 298 K, this work; ■, 313 K, this work) and CO₂ (1) + ethanol (2) (○, 298 K, Kordikowski et al.¹⁶; □, 313 K, Suzuki et al.¹⁹; ◇, Yoon et al.²⁰; ▽, Jennings et al.²¹).

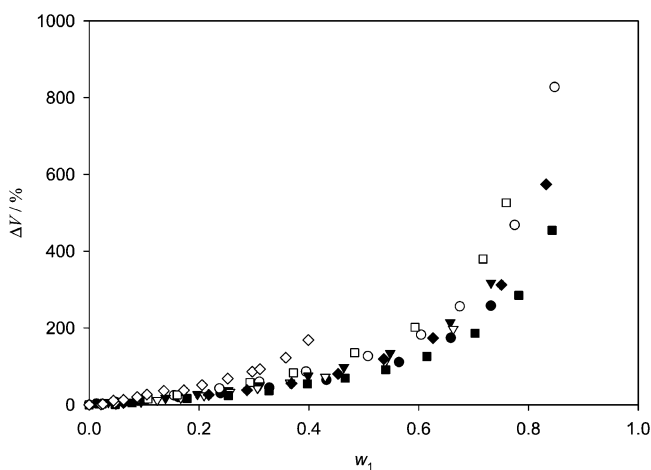


Figure 8. Percent volume change vs weight fraction of CO₂ of carbon dioxide (1) + organic solvent (2) at 313 K: ●, 2-propanol; ○, TFE; ▼, nitromethane; ▽, NMP; ■, acetonitrile; □, dichloromethane; ◆, THF; ◇, perfluorohexane.

tributes some dipolar character to it. A solubility comparison in ethanol versus 2,2,2-trifluoroethanol, as shown in Figure 7, reveals that CO₂ is less soluble in the less polar, hydrogen-bonded ethanol than the more polar, unassociated 2,2,2-trifluoroethanol.

The change in volume upon the addition of CO₂ to an organic solvent is obviously dependent upon the density of the solvent. As can be seen in Figure 8, the rate of volume expansion versus mass fraction of CO₂ in the liquid phase is most rapid with very dense solvents such as perfluorohexane (1.67 g/cm³), less so with dichloromethane (1.29 g/cm³), and slowest with acetonitrile (0.76 g/cm³). This agrees with Francis¹² in that CO₂ tends to add to organic liquids with a partial molar density of around (1.0 to 1.1) g/cm³.

Literature Cited

- (1) Reverchon, E.; Caputo, G.; De Marco, I. Role of Phase Behavior and Atomization in the Supercritical Antisolvent Precipitation. *Ind. Eng. Chem. Res.* **2003**, *42*, 6406–6414.
- (2) Musie, G.; Wei, M.; Subramaniam, B.; Busch, D. H. Catalytic Oxidations in Carbon Dioxide-Based Reaction Media, Including Novel CO₂-Expanded Phases. *Coord. Chem. Rev.* **2001**, *219–221*, 789.
- (3) Gläser, R.; Williardt, J.; Bush, D.; Lazzaroni, M. J.; Eckert, C. A. Application of High-Pressure Phase Equilibria to the Selective Oxidation of Alcohols Over Supported Platinum Catalysts in Supercritical Carbon Dioxide. In *Utilization of Greenhouse Gases*;

- Liu, C.-J.; Mallinson, R. G.; Aresta, M., Eds.; American Chemical Society: Washington, DC, 2003; pp 352–364.
- (4) Lu, J.; Lazzaroni, M. J.; Hallett, J. P.; Bommarius, A. S.; Liotta, C. L.; Eckert, C. A. Tunable Solvents for Homogeneous Catalyst Recycle. *Ind. Eng. Chem. Res.* **2004**, *43*, 1586–1590.
- (5) Patel, N. C.; Teja, A. S. A New Cubic Equation of State for Fluids and Fluid Mixtures. *Chem. Eng. Sci.* **1982**, *37*, 463–473.
- (6) Mathias, P. M.; Klotz, H. C.; Prausnitz, J. M. Equation of State Mixing Rules for Multicomponent Mixtures: the Problem of Invariance. *Fluid Phase Equilib.* **1991**, *67*, 31–44.
- (7) Span, R.; Wagner, W. A new equation of state for carbon dioxide covering the fluid region from the triple-point temperature to 1100 K at pressures up to 800 MPa. *J. Phys. Chem. Ref. Data* **1996**, *25*, 1509–1596.
- (8) Wilding, W. V.; Adams, K. L.; Carmichael, A. E.; Hull, J. B.; Jarman, T. C.; Jenkins, K. P.; Marshall, T. L.; Wilson, H. L. Vapor–Liquid Equilibrium Measurements on Three Binary Mixtures: Difluoromethane/Hydrogen Chloride, *cis*-1,3-Dichloropropene/*trans*-1,3-Dichloropropene, and Pyrrole/Water. *J. Chem. Eng. Data* **2002**, *47*, 748–756.
- (9) Elbaccouch, M. M.; Bondar, V. I.; Carbonell, R. G.; Grant, C. S. Phase Equilibrium Behavior of the Binary Systems CO₂ + Nonadecane and CO₂ + Soysolv and the Ternary System CO₂ + Soysolv + Quaternary Ammonium Chloride Surfactant. *J. Chem. Eng. Data* **2003**, *48*, 1401–1406.
- (10) Scurto, A. M.; Lubbers, C. M.; Xu, G.; Brennecke, J. F. Experimental Measurement and Modeling of the Vapor–Liquid Equilibrium of Carbon Dioxide + Chloroform. *Fluid Phase Equilib.* **2001**, *190*, 135–147.
- (11) de la Fuente Badilla, J. C.; Peters, C. J.; de Swaan Arons, J. Volume Expansion in Relation to the Gas–Antisolvent Process. *J. Supercrit. Fluids* **2000**, *17*, 13–23.
- (12) Francis, A. W. Ternary Systems of Liquid Carbon Dioxide. *J. Phys. Chem.* **1954**, *58*, 1099–1114.
- (13) DIPPR 801 Database; Brigham Young University: Provo, UT, 2004.
- (14) Bamberger, A.; Maurer, G. High-Pressure (Vapor + Liquid) Equilibria in (Carbon Dioxide + Acetone or 2-Propanol) at Temperatures from 293 K to 333 K. *J. Chem. Thermodyn.* **2000**, *32*, 685–700.
- (15) Im, J.; Lee, J.; Kim, H. Vapor–Liquid Equilibria of the Binary Carbon Dioxide–Tetrahydrofuran Mixture System. *J. Chem. Eng. Data* **2004**, *49*, 35–37.
- (16) Kordikowski, A.; Schenk, A. P.; Van Nielen, R. M.; Peters, C. J. Volume Expansions and Vapor–Liquid Equilibria of Binary Mixtures of a Variety of Polar Solvents and Certain Near-Critical Solvents. *J. Supercrit. Fluids* **1995**, *8*, 205–216.
- (17) Yaginuma, R.; Nakajima, T.; Tanaka, H.; Kato, M. Densities of Carbon Dioxide + 2-Propanol at 313.15 K and Pressures to 9.8 MPa. *J. Chem. Eng. Data* **1997**, *42*, 814–816.
- (18) Ohgaki, K.; Katayama, T. Isothermal Vapor–Liquid Equilibrium Data for Binary Systems Containing Carbon Dioxide at High Pressures: Methanol–Carbon Dioxide, *n*-Hexane–Carbon Dioxide, and Benzene–Carbon Dioxide Systems. *J. Chem. Eng. Data* **1976**, *21*, 53–55.
- (19) Suzuki, K.; Sue, H.; Itou, M.; Smith, R. L.; Inomata, H.; Arai, K.; Saito, S. Isothermal Vapor–Liquid Equilibrium Data for Binary Systems at High Pressures: Carbon Dioxide–Methanol, Carbon Dioxide–Ethanol, Carbon Dioxide–1-Propanol, Methane–Ethanol, Methane–1-Propanol, Ethane–Ethanol, and Ethane–1-Propanol Systems. *J. Chem. Eng. Data* **1990**, *35*, 63–66.
- (20) Yoon, J.-H.; Lee, H.-S.; Lee, H. High-Pressure Vapor–Liquid Equilibria for Carbon Dioxide + Methanol, Carbon Dioxide + Ethanol, and Carbon Dioxide + Methanol + Ethanol. *J. Chem. Eng. Data* **1993**, *38*, 53–55.
- (21) Jennings, D. W.; Lee, R.-J.; Teja, A. S. Vapor–Liquid Equilibria in the Carbon Dioxide + Ethanol and Carbon Dioxide + 1-Butanol Systems. *J. Chem. Eng. Data* **1991**, *36*, 303–307.

Received for review April 7, 2004. Accepted October 3, 2004. We are grateful for financial support from the National Science Foundation under grant CTS-0328019 (CO₂-Enhanced Aqueous Extraction for Benign Separation of Reaction Products).

JE0498560